Accepted manuscript of

Proteins as Supramolecular Hosts for C_{60}: A True Solution of C_{60} in Water

Matteo Di Giosia [a], Paul H. H. Bomans [b], Andrea Bottoni [a], Andrea Cantelli [a], Giuseppe Falini [a], Paola Franchi [a], Giuseppe Guarracino [a], Heiner Friedrich [b], Marco Lucarini [a], Francesco Paolucci [a], Stefania Rapino [a], Nico A. J. M. Sommerdijk [b], Alice Soldà [a], Francesco Valle [c], Francesco Zerbetto [a] and Matteo Calvaresi *[a]

[a]Dipartimento di Chimica "G. Ciamician", Alma Mater Studiorum – Università di Bologna, via F. Selmi 2, 40126 Bologna, Italy.

[b]Laboratory of Materials and Interface Chemistry & Centre for Multiscale Electron Microscopy Department of Chemical Engineering and Chemistry, Eindhoven University of Technology, Eindhoven 5600 MB, The Netherlands

[c]Istituto per lo Studio dei Materiali Nanostrutturati (CNR-ISMN), Consiglio Nazionale delle Ricerche, via P. Gobetti 101, 40129 Bologna, Italy

Corresponding author: e-mail: matteo.calvaresi3@unibo.it

Original Publication:
Proteins as Supramolecular Hosts for C_{60}: A True Solution of C_{60} in Water

DOI: 10.1039/C8NR02220H (Paper) Nanoscale, 2018, **10**, 9908-9916

Proteins as Supramolecular Hosts for C_{60}: A True Solution of C_{60} in Water.

Matteo Di Giosia,[a] Paul H.H. Bomans,[b] Andrea Bottoni,[a] Andrea Cantelli,[a] Giuseppe Falini,[a] Paola Franchi,[a] Giuseppe Guarracino,[a] H. Friedrich,[b] Marco Lucarini,[a] Francesco Paolucci,[a] Stefania Rapino,[a] Nico Sommerdijk,[b] Alice Soldà,[a] Francesco Valle,[c] Francesco Zerbetto[a] and Matteo Calvaresi*[a]

[a] Dipartimento di Chimica "G. Ciamician", Alma Mater Studiorum − Università di Bologna, via F. Selmi 2, 40126 Bologna, Italy

[b] Laboratory of Materials and Interface Chemistry & Centre for Multiscale Electron Microscopy Department of Chemical Engineering and Chemistry, Eindhoven University of Technology, Eindhoven 5600 MB, The Netherlands

[c] Istituto per lo Studio dei Materiali Nanostrutturati (CNR-ISMN), Consiglio Nazionale delle Ricerche, via P. Gobetti 101, 40129 Bologna, Italy

ABSTRACT

Hybrid systems have great potential for a wide range of applications in chemistry, physics and materials science. Conjugation of a biosystem to a molecular material can tune the properties of the components or make new ones arise. As a workhorse, here we take C_{60}@lysozyme hybrid. We show that lysozyme recognizes and disperses fullerene in water. AFM, Cryo-TEM and high resolution X-ray powder diffraction show that the C_{60} dispersion is monomolecular. The adduct is biocompatible, stable in physiological and technologically-relevant environments, and easily storable.

Hybridization with lysozyme preserves the electrochemical properties of C_{60}. EPR spin-trapping experiments show that the C_{60}@lysozyme hybrid produces ROS following both the type I and type II mechanisms. Due to the shielding effect of the protein, the adduct generates significant amounts of $^1O_2$ also in aqueous solution. In the case of the type I mechanism, the protein residues provide the electron and the hybrid does not require addition of external electron donors. The preparation and the properties of C_{60}@lysozyme are general and can be expected to be similar in other C_{60}@protein systems. It is envisaged that the properties of the C_{60}@protein hybrids will pave the way for a host of applications in nanomedicine, nanotechnology, and photocatalysis.

TOC

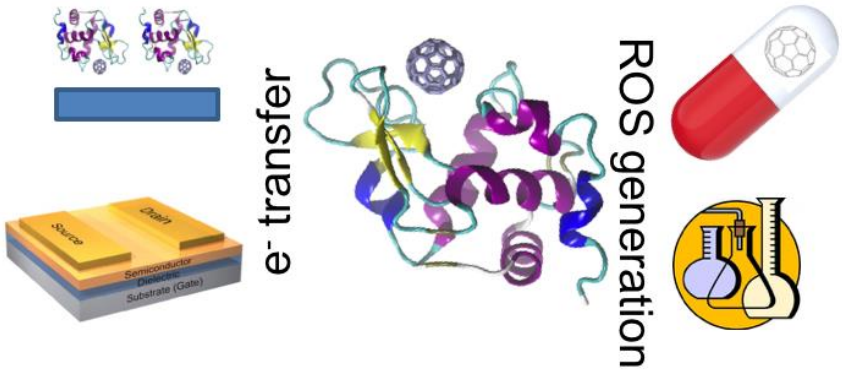

INTRODUCTION

C_{60} retains a privileged status in the carbon family and continues to stimulate the development of new platforms for producing advanced materials. Versatile technological applications of fullerenes have been proposed and are in continuous development in different fields that cover lubricants, superconductors, sensors, solar cells, pharmaceutical scaffold, contrast agents, therapeutic agents in cancer therapy, and, in general, new applications for nanotechnology[1-11] and nanomedicine.[4,12-17]

The insolubility of fullerene in a physiological environment and the formation of fullerene aggregates, also in organic solvents, hampers its exploitation.[18] The photophysical and photochemical properties of C_{60} depend strictly on the nature of the fullerene dispersion and a strict control of the dispersion is truly necessary for technological applications.[19,20]

Different approaches have been used to increase the dispersion of fullerenes, each with its own drawbacks:

i) Mechanical dispersion-stabilization of C_{60},[21] either through ultrasonication[22] or by solvent-exchange methods.[23] These mechano-physical approaches generate only metastable dispersions of fullerenes, that eventually re-aggregate. These harsh treatments may determine uncontrolled modifications of the chemical surface of C_{60}.[24]

ii) Synthesis of water-soluble fullerene derivatives by chemical functionalization with hydrophilic groups of pristine fullerene.[4,25,26] The chemical functionalization of the fullerene shows limitations due to fact that soft derivatization processes maintain the tendency of these amphiphilic C_{60} derivatives to aggregate,[27] while multiple functionalization leads to the alterations of the unique structure of fullerene and has a

negative influence on its peculiar properties; thus, restricting the potential for applications.

iii) Use of dispersants such as surfactants, block copolymers, amphiphilic polymers, micelles and liposomes.[28,29] The use of dispersants is effective and a large quantity of C_{60} can be dispersed also in water. The resulting solutions are characterized by polydispersion of fullerene aggregates of different sizes, because the fullerenes may exist in the form of both small aggregates solubilized within the hydrophobic core of the nanostructures formed by the dispersants and large aggregates stabilized by surface adsorption of the dispersants.[28,29]

iv) Dispersion of C_{60} by suitable carriers endowed with hydrophobic cores, such as γ–cyclodextrins, calixarenes, and other macrocyclic receptors or molecular tweezers.[30-32] The supramolecular approach is the most effective way to obtain monodispersed pristine fullerenes. Subsequent aggregation of the inclusion complexes[33] is common and for some biological application the fullerene host may be toxic.

Many proteins are known to interact with fullerenes.[34-66] Few are the studies that aim to exploit the protein-C_{60} recognition process for technological application. When proteins were used to disperse fullerene in water, they were simply used in lieu of surfactant molecules,[67,68] leading to fullerene aggregates of various sizes.[67,68] We recently proposed an innovative approach, using a protein, namely lysozyme, to disperse with a 1:1 stoichiometry C_{60}.[36,44] The recognition is well-defined and the fullerene binds selectively in the protein substrate binding pocket.[36,44] Lysozyme, as many proteins, follows, as a supramolecular host, the set of rules defined by Martin and Perez[69,70] to recognize efficiently carbon nanomaterials[36,71] which entail i) the presence of a nonpolar cavity, featuring aromatic recognizing units (Trp residues), of

the appropriate size to fit the fullerene cage; ii) a recognition process based on concave-convex complementarity; iii) a high degree of pre-organization of the host (due to the 3D structure of the protein) that lowers the entropic cost for guest binding.

RESULTS AND DISCUSSION

C_{60}@lysozyme hybrids were prepared in an Eppendorf by adding C_{60} powder in a solution of lysozyme. The Eppendorf was ultrasonicated and after centrifugation and collection of the supernatant, a brown solution was obtained. UV-vis spectrum of the solution (Figure 1) clearly demonstrates the presence of fullerene in water, in particular notice the diagnostic band at 341 nm. This dispersion system is more efficient that the commonly used γ-cyclodextrin, that represents the most popular way to disperse C_{60} in water (Figure 1). The absorbance at 341 nm for C_{60}@lysozyme (0.515) is 1.76 higher than C_{60} dispersed with γ-cyclodextrin (0.293).

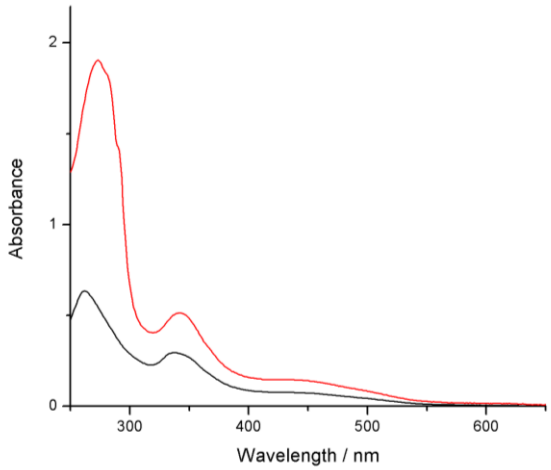

Figure 1. UV-visible spectra of C_{60}@lysozyme hybrids (red line) and C_{60}@2γ-cyclodextrin (black line).

AFM Imaging of C_{60}@Lysozyme hybrids. NMR experiments have already shown the formation of a 1:1 stoichiometric adduct between lysozyme and the fullerene.[36] A

direct measure of the dispersion of the C_{60}@lysozyme hybrid is provided by atomic force microscopy (AFM). In Figure 2a the C_{60}@lysozyme hybrids appear monomoleculary dispersed over a mica surface. Height distribution analysis (Figure 2b) of the AFM images is consistent with that of a singly adsorbed C_{60}@lysozyme monodispersed and confirms the lack of presence of C_{60}@lysozyme aggregates, or nC_{60} aggregates dispersed by the protein.

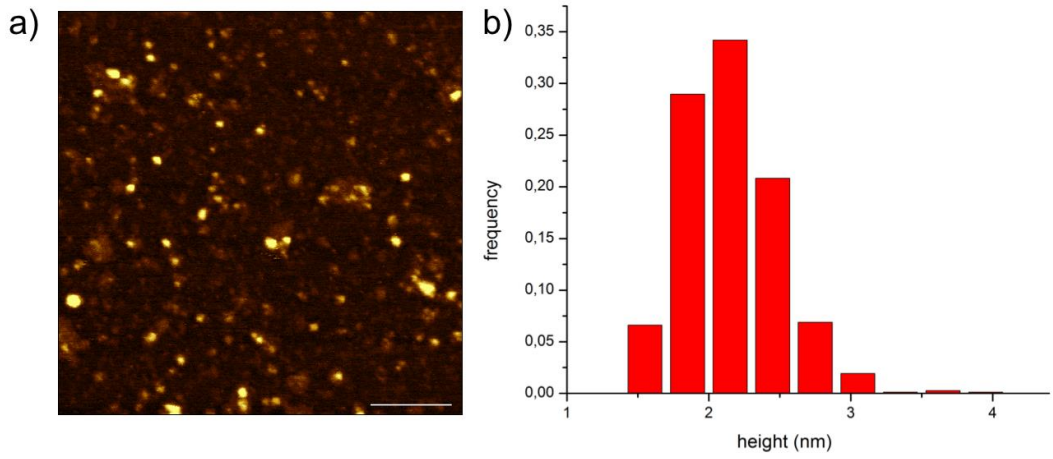

Figure 2. a) AFM image of C_{60}@lysozyme, top view (500 nm x 500 nm), scale bar 100 nm; b) Height distribution analysis of the AFM images.

To eliminate possible surface-effects due to adsorption of proteins on a surface, cryo-TEM experiments were carried out on the C_{60}@lysozyme solution. Cryo-TEM images allowed direct visualization of the dispersion state in solution of the C_{60}@lysozyme hybrids (Figure 3a).[72] The particle size distribution (Figure 3b) shows that the C_{60}@lysozyme are monodispersed and there is no presence of nC_{60} aggregates. These aggregates were previously observed when proteins or other surfactants were used as dispersants. They showed faceted, high-contrast particles, characteristic of crystalline aggregates.[68,69,73]

Furthermore, when fullerene aggregates (nC_{60}) are present in solution, X-ray

diffraction patterns show peaks that evidence the presence of crystalline aggregates of fullerene.[74,75] The high resolution X-ray powder diffraction pattern of a freeze-dried C_{60}@lysozyme solution does not show any diffraction peak (Figure 3c).

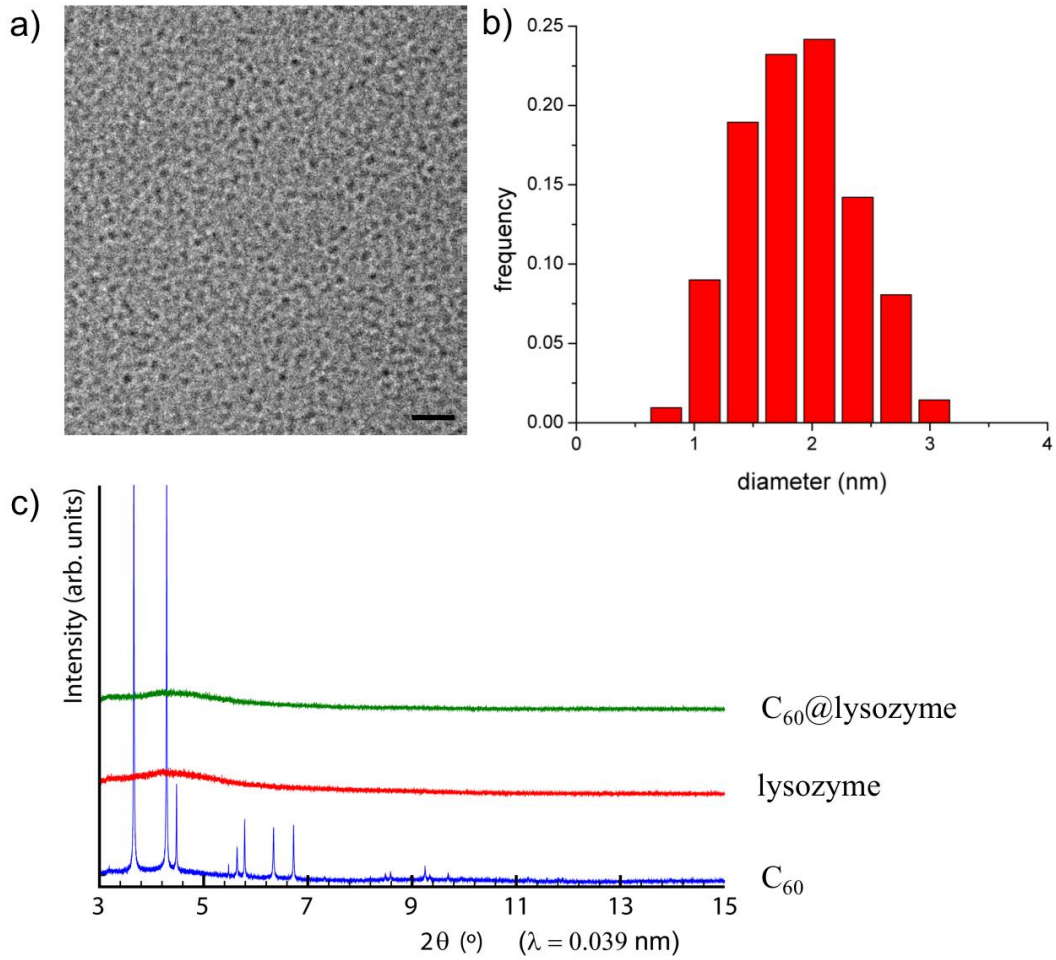

Figure 3. a) Cryo-TEM image of C_{60}@lysozyme solution, scale bar 20 nm; b) Particle size distribution of the C_{60}@lysozyme; c) High resolution X-ray powder diffraction of C_{60} (blue line), lysozyme (red line) and C_{60}@lysozyme (green line).

These data confirm the absence of C_{60} crystalline aggregates in solution, the ability of lysozyme to disperse monomolecularly C_{60} and more importantly provide a route for the storage of monodispersed fullerene by lyophilization. In fact, re-dissolution of the lyophilized powder gives back a solution with the same characteristic of the starting

C_{60}@lysozyme solution.

Stability of C60@lysozyme hybrids. The analysis of the stability of C_{60}@lysozyme at different pH's shows that the solution is stable up to the isoelectric point of lysozyme (pH 10.7), where aggregation occurs (Figure 4a).

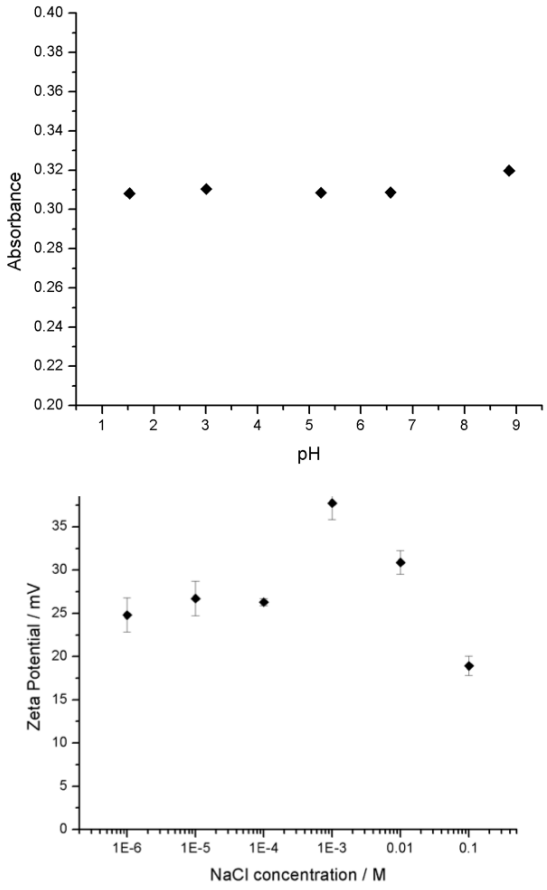

Figure 4. C_{60}@lysozyme: a) Absorbance vs pH; b) zeta potential at different NaCl concentrations.

The C_{60}@lysozyme adduct is stable also at different saline concentrations, up to physiological concentration (Figure 4b), while usually C_{60} dispersed by γ-cyclodextrins or nC_{60} rapidly precipitates when NaCl is added.[23] This mean that the C_{60} solubility is governed entirely by the protein. The solutions of C_{60}@lysozyme remain stable for months in water. The formation of monodispersions and stability of

C_{60}@lysozyme, in water and in saline solutions, open the way for technological applications able to exploit the chemical-physics properties of C_{60} in physiological and technological relevant environments.

Electrochemical characterization of C_{60}@lysozyme hybrids

In Figure 5a the cyclic voltammetry recorded for the C_{60}@lysozyme hybrids and for lysozyme are shown.

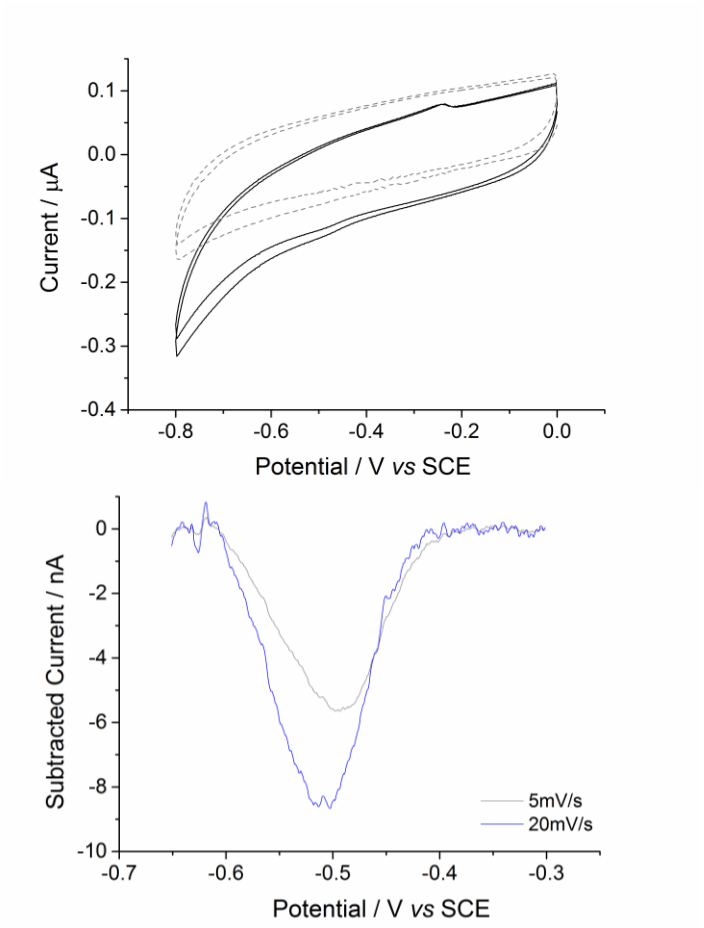

Figure 5. a) Cyclic voltammograms of C_{60}@lysozyme hybrids (bold line) and pristine lysozime (dashed line), scan rate 5 mV/s. b) C_{60}@lysozyme reduction peak baselines subtracted scan rate 5 mV/s (gray line), 20mV/s (blue line). A glassy carbon was used as working electrode in 10 mM NaCl aqueous solution, the potentials are reported towards SCE reference electrode.

C_{60}@lysozyme shows a reduction peak at -0.49 V vs SCE and an oxidation peak at -0.24 V vs SCE. No peaks were observed in the same potential window for the pristine lysozyme. The peak-peak separation is 250 mV in accordance with a slow charge transfer probably due to the hindrance of the C_{60} charge transfer to the electrode caused by the protein. In Figure 5b, the reduction peaks of C_{60}@lysozyme, subtracted for the baseline recorded at 5 and 20 mV/s, are reported. The potential of the reduction peak is around -0.5 V vs SCE. This potential is more negative than the one recorded for C_{60} in organic solvent, a behavior that is due to the partial charge transfer of the amino acids constituting the binding site to the C_{60} moiety. We already showed that two tryptophan residues tightly interact with the C_{60} cage in the binding site[36] and that they establish a charge transfer process toward C_{60}.[36]

C_{60} presents six possible reduction waves, anyway they are only rarely observed in ultra-dry solvents, typically 2-3 quasi-reversible reduction waves are observed in organic solvents. Here, we report for the first time the electrochemical behaviour of a C_{60}@protein complex monodispersed in water, which retain the first reduction wave of C_{60}. This process appears to be irreversible in the investigated conditions. The voltammetric study confirms that the first reduction of C_{60} is observable even when the carbon cage is confined in the protein binding pocket. In turn, modification of the pocket may tune C_{60} redox potential. Since fullerenes are ideal electron mediators, C_{60}@protein hybrids can lead to new applications of C_{60} in electrochemical catalytic systems or in biosensing.[10-12]

Photoinduced reactive oxygen species (ROS) generation by C_{60}@lysozyme hybrids

C_{60} shows a significant visible light-induced generation of ROS, that can be exploited in photodynamic therapy[76-87] or photocatalysis.[88-91] However, the use of C_{60} molecules in water still presents important restrictions in its application due to both the dependency of C_{60} properties on the physiological environment and the related aggregation phenomena[92] and C_{60} poor solubility.[18] Aggregation is a well-known factor that deactivates the electronically excited states of photosensitizers, drastically decreasing the long-lived triplet excited state lifetime, and consequently reducing the ROS production efficiency.[19,20,92,93] When fullerene aggregates are present, $^3C_{60}{}^*$ is rapidly quenched by the surrounding C_{60} or by other $^3C_{60}{}^*$.[20] In addition, aggregation reduces the active surface area of C_{60} in contact with oxygen molecules for ROS production. The possibility to use C_{60}@lysozyme may overcome the current limitations.

Two different pathways can be identified for the production of ROS upon light absorption by C_{60}. In the simpler pathway (also known as type II energy transfer), the singlet excited state of C_{60}, initially formed, is converted to the long lived triplet state through intersystem crossing with a quantum yield close to unity. $^3C_{60}$ can be efficiently quenched by molecular oxygen ($^3O_2$) to generate large amounts of singlet oxygen ($^1O_2$). In the more complex pathway (also known as type I electron transfer), $^3C_{60}$ in the presence of electron donors gives the C_{60} radical anion that can readily transfer the electron to molecular oxygen forming the superoxide anion radical ($O_2^{-\bullet}$) or hydroxyl radical ($^\bullet$OH). EPR measurements with the use of a spin trap can be used to verify the presence of the two pathways.

$^1O_2$ production was detected by EPR using 2,2,6,6-tetramethyl-4-piperidone (4-oxo-TEMP) as a probe. Actually, 4-oxo-TEMP reacts with $^1O_2$ to afford 4-oxo-TEMPO nitroxide radical (see Figure 6a) that can be detected by EPR. The measurements were

carried out by irradiating with visible light the aqueous solution containing lysozyme, C_{60}@lysozyme, and C_{60}@2γ-cyclodextrin. All solutions were prepared at the same fullerene concentration (identified by same intensity of absorption at 341 nm). When lysozyme and C_{60}@2γ-cyclodextrin were irradiated up to 15 minutes in the presence of 4-oxo-TEMP no significant increase of the signal due to 4-oxo-TEMPO was detected by EPR. On the contrary, the specific signals of 4-oxo-TEMPO significantly increases when C_{60}@lysozyme is photoirradiated for 15 min (see Figure 6b). This result suggests that a significant amount of $^1O_2$ is generated in the aqueous solution during irradiation of C_{60}@lysozyme and that the protein environment strongly reduces the quenching of the singlet oxygen by water molecules.

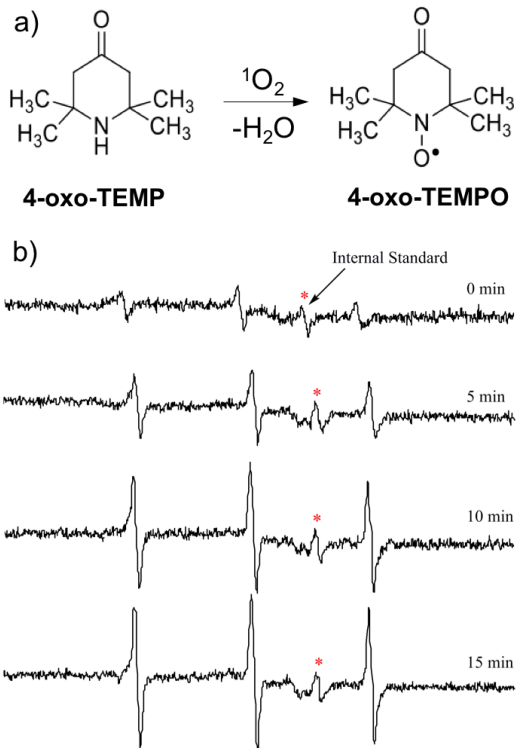

Figure 6. a) Reaction scheme for the generation of 4-oxo-TEMPO by the reaction of $^1O_2$ with 4-oxo-TEMP; b) X-band EPR spectra of 4-oxo-TEMPO formed in aqueous solution of C_{60}@lisozyme complex at different irradiation times.

The pathway for ROS generation was also investigated by using EPR with 5,5-dimethyl-1-pyrroline-N-oxide (DMPO) as a spin-trapping reagent. The generation of ·OH was detected through an EPR signal corresponding to DMPO-OH, formed by the reaction of ·OH with DMPO (figure 7a).

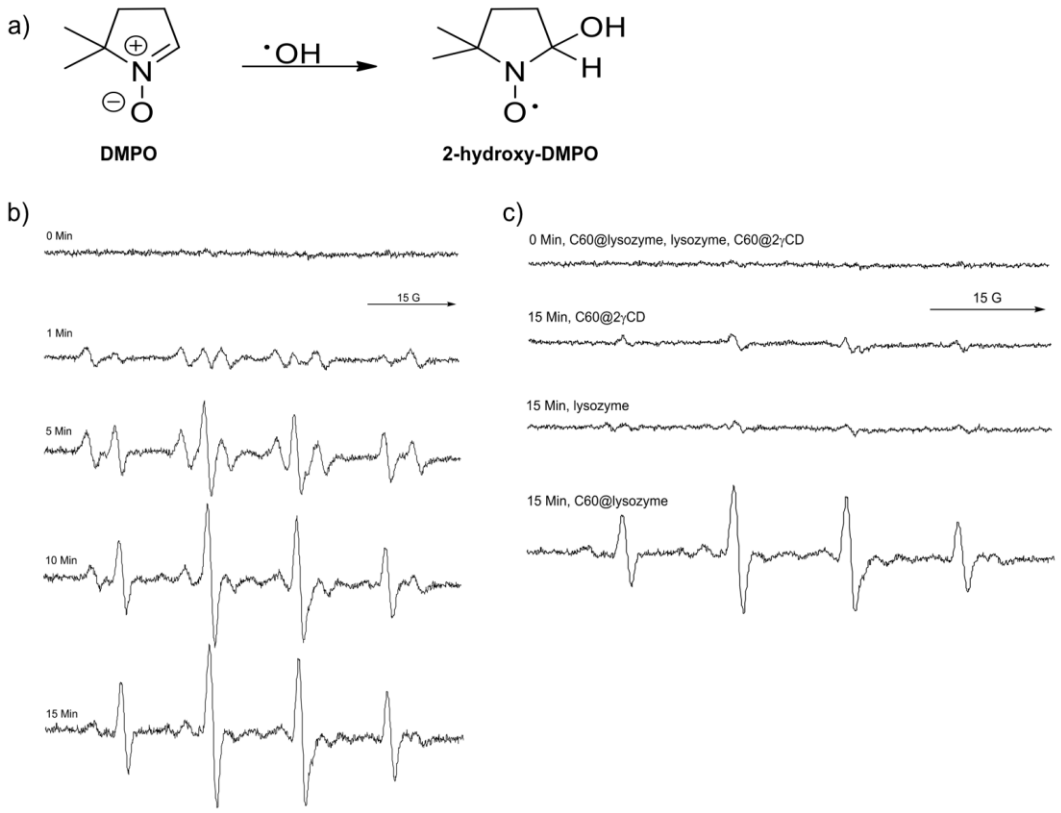

Figure 7. a) Reaction scheme for the generation of DMPO-OH by the reaction of ·OH with DEMPO; b) X-band EPR spectra of DMPO-OH formed in aqueous solution of C_{60}@lisozyme complex at different irradiation times; c) X-band EPR spectra of DMPO-OH at time 0 and after 15 minutes of photoirradiation for C_{60}@2γ-cyclodextrin, lysozyme and C_{60}@lysozyme.

Figure 7b shows clearly the specific signals of DMPO-OH (a_N=a_H=14.75 G), which was produced upon irradiation by the reaction of DMPO with the radical oxygen species generated by C_{60}@lysozyme. During the initial minutes of irradiation, the spectrum shows also the presence of an alkyl adduct to DMPO (a_N = 15.80 G, a_H =

22.52 G). Extension of irradiation, however, leads to a significant decrease in the intensity of this signal.

With C_{60}@2γ-cyclodextrin or lysozyme the amount of radical oxygen species generated by irradiation of the aqueous solution was significantly smaller, as indicated by the very weak EPR signal recorded in these conditions (figure 7c).

Importantly, in the case of the type I mechanism, measurements involving C_{60} need the addition of a sacrificial electron donor, as for example NADH or triethylamine. C_{60}@lysozyme hybrid, however, does not need any external electron donors because the protein residues do this work. This means that the type I mechanism is self-activated in the C_{60}@lysozyme hybrid, due to the presence of the protein itself.

The high performances of C_{60}@lysozyme in the visible light-induced generation of ROS in water suggest the potential use of this hybrid as an agent for photodynamic therapy.[76-87] Photogenerated singlet oxygen can be used also in synthetic organic chemistry. Even though singlet oxygen is a short-lived metastable excited state of molecular oxygen, it is a practical reagent for compound oxidation and can form carbon-oxygen and heteroatom-oxygen bonds.[88-91]

CONCLUSION

In this paper we demonstrated that lysozyme can be used as a host molecule to recognize and disperse fullerene in water. AFM, Cryo-TEM and high resolution X-ray powder diffraction showed that the C_{60} dispersion is monomolecular. The adduct is biocompatible, stable in physiological and technologically-relevant environments, and easily storable. The electrochemical properties of C_{60} are preserved in the C_{60}@proteins hybrid suggesting new applications in electrochemical catalytic systems, biosensing or bioelectronics. EPR spin-trapping experiments showed that the

C_{60}@lysozyme hybrid is able to produce a considerable amount of ROS following both the type I and type II mechanism. This behavior suggests potential application of C_{60}@proteins in photodynamic therapy or in organic synthesis as singlet oxygen generator. Considering the use of C_{60} in nanomedicine, C_{60}@proteins hybrids may be also potentially used for sonodynamic therapy, enhanced microwave and radiowave induced hyperthermia, photothermal treatment and optoacoustic imaging.

In addition, the different chemical groups offered by the protein platform allow an easy route for the functionalization of the hybrid, without altering the structure and properties of fullerene. C_{60}@protein hybrids could be augmented by using 1) targeting tags able to improve the cell/bacterial selectivity and promote the uptake of the C_{60}@proteins hybrid in cancer or antimicrobial therapy; 2) imaging tags to create an innovative, protein based theranostic platform; 3) light-harvesting antennae to extend the absorption spectrum of the C_{60}@proteins hybrid further into the red. Furthermore, these hybrids could be used to create stable and ordered C_{60} suprastructures on surfaces with potential applications in nanotechnology, ranging from sensors and photovoltaic cells to nanostructured devices for advanced electronic applications.

Proteins other than lysozyme can be exploited in the future to tune the C_{60} properties[94] and to shape a variety of C_{60} spatial arrangements on surfaces, controlling the C_{60} molecular assembly. C_{60} has not yet exhausted its role as a leading material, because its integration in biomolecules will pave the way to new innovative applications.

MATERIALS AND METHODS

Synthesis of C_{60}@lysozyme and C_{60}@2γ-cyclodextrin hybrids.

The adduct of C_{60}@2γ-cyclodextrin and C_{60}@lysozyme was synthesized as described previously.[36] C_{60} powder (Sigma-Aldrich, Cat. no. 483036) was used in 2:1 excess

with respect to the stoichiometric relationship to 1 mL of a 1 mM solution of lysozyme (lysozyme from chicken egg white lyophilized powder, Cat. no. L6876) or γ-cyclodextrin (Sigma-Aldrich, Cat. no. C4892) in Milli-Q water. After sonication for 60 min using a probe tip sonicator (Hielscher Ultrasonic Processor UP200St, equipped with a sonotrode S26d7, used at 45% of the maximum amplitude) in an ice bath, C_{60} was dispersed in the solution forming a dark brown mixture. A dark-brown solution was obtained after centrifugation at 10 600g for 10 min and the supernatant was collected. In order to eliminate possible ROS generated during the sonication process, the solution has been washed four times with the 3K Amicon Ultra-0.5 Centrifugal Filter Units, using a volume of 500 mL and spinning at 14 000 g for 20 minutes, obtaining a concentration factor of 8. After each spin the volume of the concentrated solution has been brought back to its original value using Milli-Q water. UV-vis absorption spectra were recorded at 25 C° by means of Agilent Cary 60 UV-Vis Spectrophotometer. Zeta potential measurements were carried out using a Malvern Zetasizer Nano ZS.

AFM measurements. AFM experiments were performed at the SPM@ISMN microscopy facility in Bologna. AFM (Digital Instruments, Multimode VIII equipped with a Nanoscope V) operated in ScanAsyst mode was used to analyze the dispersion state of the proteins. The samples for AFM measurements were prepared by drop casting 5 μl of C_{60}@lysozyme hybrids solution onto a freshly cleaved mica substrate for 10 min then rinsed with milliQ water and dried with a stream of N_2. Height distribution from AFM images was calculated using Gwyddion.

Cryo-TEM microscopy. Sample vitrification was performed using an automated vitrification robot (FEI Vitrobot™ Mark III) for plunging in liquid ethane. TEM Cu Quantifoil grids, R2/2 (Quantifoil Micro Tools GmbH) were surface plasma cleaned for

40 s using a Cressington 208 carbon coater prior to use. The samples were studied on the TU/e Cryo Titan (FEI, http://www.cryotem.nl), equipped with a field emission gun (FEG) operating at 300 kV and a post column Gatan energy filter (GIF). Images were recorded using a post-GIF 2k x 2k Gatan CCD camera in low dose conditions. Particle diameters were measured with the Measure_lengths script from the CMEM toolbox. As spherical symmetry was assumed, the diameter was averaged over the 'length' and the 'width'. For each image, 6 regions were selected, in which approx. 33 particles were measured. Data was analyzed with Origin. The data was binned in bins with sizes set equal to the pixel size (0,2814 nm).

X-ray powder diffraction measurements. High resolution X-ray powder diffraction (HRPXRD) measurements were collected with a dedicated high-resolution powder diffraction synchrotron beamline (ID22 at the European Synchrotron Radiation Facility (ESRF), Grenoble, France) using as wavelength 0.039 nm. The C_{60}@protein water dispersions were lyophilized before the HRPXRD measurements.

Electrochemical characterization of C_{60}@lysozyme hybrids.

Instrumentation. The electrochemical measurements were performed using a CHI900B bipotentiostat (from CH Instruments Inc. Austin, TX) in a typical three-electrode configuration cell. A glassy carbon (ø = 1 mm) was used as working electrode (WE), a platinum wire as counter electrode (CE) and a saturated calomel electrode (SCE) as reference electrode (RE). The working electrode was carefully polished before its use by mechanical polishing employing 0.05 mm alumina paste and successively cleaned ultrasonically in distilled water for 5 min.

Measurement. The solution (PBS 1x) was degassed by bubbling Ar for at least 30 min before measuring and the cyclic voltammetry was carried out by cycling the

potential range from 0.0 to -0.8 V at different scan rate: 5 mV/s– 10mV/s – 20mV/s – 50mV/s – 100mV/s.

EPR spectroscopy. EPR spectra were recorded at 298 K using an ELEXYS E500 spectrometer equipped with an NMR gaussmeter for the calibration of the magnetic field and a frequency counter for the determination of g-factors that were corrected against that of the perylene radical cation in concentrated sulfuric acid (g = 2.002583). Light irradiation and EPR measurements were carried out on the sample in a capillary tubes (1 mm i.d.). Measurement conditions: modulation amplitude = 1.0 G; conversion time = 163.84 ms; time constant = 163.84 ms; modulation frequency 100 kHz; microwave power = 6.4 mW; microwave frequency 9.375 GHz.

$^1O_2$ generation by the EPR spin-trapping method. $^1O_2$ was detected by EPR using 2,2,6,6-tetramethyl-4-piperidone (4-oxo-TEMP, Sigma-Aldrich, Cat. no. 459119) as probe. To 0.1 mM C_{60}@lysozyme (40 μL) in milliQ water, 0.5 M 4-oxo-TEMP (20 μL), and milliQ water (140 μL) were added and mixed well. The mixed solution was introduced into a capillary tube, deaerated under nitrogen flux, sealed and placed inside an EPR tube. The sample was irradiated by a UV-filtered 500 W high pressure mercury lamp and subjected to EPR measurements. The generation of singlet oxygen was detected by the three line EPR signal (a_N= 16.13 G) corresponding to 4-oxo-TEMPO, formed by the reaction of $^1O_2$ with 4-oxo-TEMP.

$^{\cdot}OH$ generation by the EPR spin-trapping method. $^{\cdot}OH$ was detected by EPR using 5,5-dimethyl-1-pyrroline-N-oxide (DMPO, Sigma-Aldrich, Cat. no. 92688) as a spin-trapping reagent. To a 0.1 mM C_{60}@lysozyme (40 μL) in milliQ water (20 μL), 0.1 mM DMPO (2 μL), and milli Q water (180 μL) were added and mixed well. The mixed solution was introduced into a capillary tube, deaerated under nitrogen flux,

sealed and placed inside an EPR tube. The sample was irradiated by a UV-filtered 500 W high pressure mercury lamp and subjected to EPR measurements. The generation of $^{\cdot}OH$ was detected as five line signal corresponding to DMPO-OH, formed by the reaction of $^{\cdot}OH$ with DMPO ($a_N = a_H = 14.75$ G).

AUTHOR INFORMATION

Corresponding Author

* matteo.calvaresi3@unibo.it

ACKNOWLEDGMENTS

The authors thank the ESRF (ID22) and Prof. Boaz Pokroy for the collection and analysis of high-resolution X-ray powder diffraction data. This study was supported by the Italian Ministry of Education, University and Research (MIUR) SIR Programme no. RBSI149ZN9-BIOTAXI funded to MC.

REFERENCES

1 M. Prato, *J. Mater. Chem.*, 1997, **7**, 1097-1109.

2 F. Wudl, *J. Mater. Chem.*, 2002, **12**, 1959-1963.

3 A. Montellano López, A. Mateo-Alonso and M. Prato, *J. Mater. Chem.*, 2011, **21**, 1305-1318.

4 E. Nakamura and H. Isobe, *Acc. Chem. Res.*, 2003, **36**, 807-815.

5 D. M. Guldi, B. M. Illescas, C. M. Atienza, M. Wielopolski and N. Martín, *Chem. Soc. Rev.*, 2009, **38**, 1587-1597.

6 D. Bonifazi, O. Enger and F. Diederich, *Chem. Soc. Rev.*, 2007, **36**, 390-414.

7 S. S. Babu, H. Möhwald and T. Nakanishi, *Chem. Soc. Rev.*, 2010, **39**, 4021-4035.

8 L. K. Shrestha, Q. Ji, T. Mori, K. Miyazawa, Y. Yamauchi, J. P. Hill and K. Ariga, *Chem. An Asian J.*, 2013, **8**, 1662-1679.

9 S. Kirner, M. Sekita and D. M. Guldi, 25th Anniversary Article: 25 Years of Fullerene Research in Electron Transfer Chemistry. *Adv. Mater.*, 2014, **26**, 1482-1493.

10 B. S. Sherigara, W. Kutner, and F. D'Souza, *Electroanalysis*, 2003, **15**, 753-772.

11 J.-F. Nierengarten, *New J. Chem.*, **2004**, *28*, 1177-1191.

12 S. Goodarzi, T. Da Ros, J. Conde, F. Sefat and M. Mozafari, *Mater. Today*, 2017, **20**, 460-480.

13 E. Castro, A. H. Garcia, G. Zavala and L. Echegoyen, *J. Mater. Chem. B*, 2017, **5**, 6523-6535.

14 A. Dellinger, Z. Zhou, J. Connor, A. Madhankumar, S. Pamujula, C. M. Sayes and C. L. Kepley, *Nanomedicine*, 2013, **8**, 1191-1208.

15 R. Partha and J. L. Conyers, *Int. J. Nanomedicine*, 2009, **4**, 261.

16 S. Bosi, T. Da Ros, G. Spalluto and M. Prato, *Eur. J. Med. Chem.*, 2003, **38**, 913-923.

17 A. Montellano, T. Da Ros, A. Bianco and M. Prato, *Nanoscale*, 2011, **3**, 4035-4041.

18 N. O. McHedlov-Petrossyan, *Chem. Rev.*, 2013, **113**, 5149-5193.

19 D. M. Guldi, H. Hungerbuehler and K.-D. Asmus, *J. Phys. Chem.*, 1995, **99**, 9380-9385.

20 D. M. Guldi and M. Prato, *Acc. Chem. Res.*, 2000, **33**, 695-703.

21 S. Deguchi, S. Mukai, M. Tsudome and K. Horikoshi, K. *Adv. Mater.*, 2006, **18**, 729-732.

22 G. V. Andrievsky, M. V. Kosevich, O. M. Vovk, V. S. Shelkovsky and L. A. Vashchenko, *J. Chem. Soc. Chem. Commun.*, 1995, **0**, 1281-1288.

23 S. Deguchi, R. G. Alargova and K. Tsujii, *Langmuir*, 2001, **17**, 6013-6017.

24 B. Todorović Marković, V. Jokanović, S. Jovanović, D. Kleut, M. Dramićanin and Z. Marković, *Appl. Surf. Sci.*, 2009, **255**, 7537-7541.

25 A. Hirsch, *Angew. Chemie Int. Ed.*, 1993, **32**, 1138-1141.

26 A. Hirsch and M. Brettreich, *Fullerenes: Chemistry and Reactions*; Wiley-VCH Verlag GmbH & Co. KGaA: Weinheim, Germany, 2005.

27 D. M. Guldi, F. Zerbetto, V. Georgakilas and M. Prato, *Acc. Chem. Res.*, 2005, **38**, 38-43.

28 V. M. Torres, M. Posa, B. Srdjenovic and A. L. Simplício, *Colloids Surf. B Biointerfaces*, 2011, **82**, 46-53.

29 M. Dallavalle, M. Leonzio, M. Calvaresi and F. Zerbetto, *ChemPhysChem*, 2014, **15**, 2998-3005.

30 D. Canevet, E. M. Pérez and N. Martín, *Angew. Chemie Int. Ed.*, 2011, **50**, 9248-9259.

31 L. Moreira, J. Calbo, R. M. K. Calderon, J. Santos, B. M. Illescas, J. Arago, J.-F. Nierengarten, D. M. Guldi, E. Orti and N. Martin, *Chem. Sci.*, **2015**, *6*, 4426-4432.

32 E. M. Pérez and N. Martín, *Pure Appl. Chem.*, 2010, **82**, 523-533.

33 M. Konstantaki, E. Koudoumas, S: Couris, J. Janot, H. Eddaoudi, A. Deratani, P. Seta and S. Leach, *Chem. Phys. Lett.*, 2000, **318**, 488-495.

34 L. Ahmed, B. Rasulev, S. Kar, P. Krupa, M. A. Mozolewska and J. Leszczynski, *Nanoscale*, 2017, **9**, 10263-10276.

35 M. Calvaresi and F. Zerbetto, *ACS Nano* 2010, **4**, 2283-2299.

36 M. Calvaresi, F. Arnesano, S. Bonacchi, A. Bottoni, V. Calò, S. Conte, G. Falini, S. Fermani, M. Losacco, M. Montalti, G. Natile, L. Prodi, F. Sparla and F. Zerbetto, *ACS Nano*, 2014, **8**, 1871-1877.

37 K.-H. Kim, D.-K. Ko, Y.-T. Kim, N. H. Kim, J. Paul, S.-Q. Zhang, C. B. Murray, R. Acharya, W. F. DeGrado, Y. H. Kim and G. Grigoryan *Nat. Commun.*, 2016, **7**, 11429.

38 A. Giełdoń, M. M. Witt, A. Gajewicz and T. Puzyn, *Struct. Chem.*, 2017, **28**, 1775-1788.

39 Y. Liu, B. Yan, D. A. Winkler, J. Fu and A. Zhang, *ACS Appl. Mater. Interfaces*, 2017, **9**, 18626-18638.

40 F. Trozzi, T. D. Marforio, A. Bottoni, F. Zerbetto and M. Calvaresi, *Isr. J. Chem.*, 2017, **57**, 547-552.

41 T. A. Hilder, A. Robinson and S.-H. Chung, *ACS Chem. Neurosci.*, 2017, **8**, 1747-1755.

42 S. J. Vance, V. DesaiB. O. Smith, M. W. Kennedy and A. Cooper, *Biophys. Chem.*, 2016, **214-215**, 27-32.

43 Y. Pan, L. Wang, S. Kang, Y. Lu, Z. Yang, T. Huynh, C. Chen, R. Zhou, M. Guo and Y. Zhao, *ACS Nano*, 2015, **9**, 6826-6836.

44 M. Calvaresi, A. Bottoni and F. Zerbetto, *J. Phys. Chem. C*, 2015, **119**, 28077-28082.

45 S. Zanzoni, A: Ceccon, M. Assfalg, R. K. Singh, D. Fushman and M. D'Onofrio, *Nanoscale*, 2015, **7**, 7197-7205.

46 Y. Miao, J. Xu, Y. Shen, L. Chen, Y. Bian, Y. Hu, W. Zhou, F. Zheng, N. Man, Y. Shen, Y. Zhang, M. Wang and L. Wen, *ACS Nano*, 2014, **8**, 6131-6144.

47 P. Chen, S. A. Seabrook, V. C. Epa, K. Kurabayashi, A. S. Barnard, D. A. Winkler, J. K. Kirby and P. C. Ke, *J. Phys. Chem. C*, 2014, **118**, 22069-22078.

48 E. Mentovich, B. Belgorodsky, M. Gozin, S. Richter and H. Cohen, *J. Am. Chem. Soc.*, 2012, **134**, 8468-8473.

49 S. Kang, G. Zhou, P. Yang, Y. Liu, B. Sun, T. Huynh, H. Meng, L. Zhao, G. Xing, C. Chen, Y. Zhao and R. Zhou, *Proc. Natl. Acad. Sci. USA*, 2012, **109**, 15431-15436.

50 M. Zhen, J. Zheng, L. Ye, S. Li, C. Jin, K. Li, D. Qiu, H. Han, C. Shu, Y. Yang and C. Wang, *ACS Appl. Mater. Interfaces*, 2012, **4**, 3724-3729.

51 T. A. Ratnikova, P. Nedumpully Govindan, E. Salonen and P. C. Ke, *ACS Nano*, 2011, 5, 6306-6314.

52 M. Calvaresi and F. Zerbetto, *Nanoscale*, 2011, **3**, 2873-2881.

53 S. Maoyong, J. Guibin, Y. Junfa and W. Hailin, *Chem. Commun.*, 2010, **46**, 1404.

54 H. Geng, Y.-N. Chang, X. Bai, S. Liu, Q. Yuan, W. Gu, J. Li, K. Chen, G. Xing and G. Xing, *Nanoscale*, *2017*, **9**, 12516-12523.

55 A. Innocenti, S. Durdagi, N. Doostdar, T. A. Strom, A. R. Barron and C. T. Supuran, *Bioorg. Med. Chem.*, 2010, **18**, 2822-2828.

56 S. Durdagi, C. T. Supuran, T. A. Strom, N. Doostdar, M. K. Kumar, A. R. Barron, T. Mavromoustakos and M. G. Papadopoulos, *J. Chem. Inf. Model.*, 2009, **49**, 1139-1143.

57. M. Turabekova, B. Rasulev, M. Theodore, J. Jackman, D. Leszczynska and J. Leszczynski, *Nanoscale*, 2014, **6**, 3488-3495

58 S.-T. Yang, H. Wang, L. Guo, Y. Gao, Y. Liu, A. Cao, *Nanotechnology*, 2008, **19**, 395101.

59 X. Wu, S. T. Yang, H. Wang, L. Wang, W. Hu, A. Cao, Y. Liu, *J. Nanosci. Nanotechnol.*, 2010, **10**, 6298-6304.

60 G. Pastorin, S. Marchesan, J. Hoebeke, T. Da Ros, L. Ehret-Sabatier, J.-P. Briand, M. Prato and A. Bianco, *Org. Biomol. Chem.*, 2006, **4**, 2556-2562.

61 X. Yin, L. Zhao, S. Kang, J. Pan, Y. Song, M. Zhang, G. Xing, F. Wang, J. Li, R. Zhou and Y. Zhao, *Nanoscale*, 2013, **5**, 7341-7348.

62 B. Belgorodsky, L. Fadeev, J. Kolsenik and M. Gozin, *ChemBioChem*, 2006, **7**, 1783-1789.

63 B. Belgorodsky, L. Fadeev, V. Ittah, H. Benyamini, S. Zelner, D. Huppert, A. B. Kotlyar and M. Gozin, *Bioconjug. Chem.*, 2005, **16**, 1058-1062.

64 L. Xie, Y. Luo, D. Lin, W. Xi, X. Yang and G. Wei, *Nanoscale*, 2014, **6**, 9752-9762.

65 K. H. Park, M. Chhowalla, Z. Iqbal and F. Sesti, *J. Biol. Chem.*, 2003, **278**, 50212-50216.

66 S. H. Friedman, D. L. DeCamp, R. P. Sijbesma, G. Srdanov, F. Wudl and G. L. Kenyon, *J. Am. Chem. Soc.*, 1993, **115**, 6506-6509.

67 H. Wu, L. Lin, P. Wang, S. Jiang, Z. Dai and X. Zou, *Chem. Commun.*, 2011, **47**, 10659-10661.

68 M. Siepi, J. Politi, P. Dardano, A. Amoresano, L. De Stefano, D. Maria Monti and E. Notomista, *Nanotechnology*, 2017, **28**, 335601.

69 E. M. Pérez and N. Martín, *Chem. Soc. Rev.*, 2015, **44**, 6425–6433.

70 E. M. Pérez and N. Martín, *Chem. Soc. Rev.*, 2008, **37**, 1512-1519.

71 H. Nie, H. Wang, A. Cao, Z. Shi, S.-T. Yang, Y. Yuan and Y. Liu, Nanoscale, 2011, **3**, 970-973.

72 J. J. De Yoreo and N. A. J. M. Sommerdijk, *Nat. Rev. Mater.*, 2016, **1**, 16035.

73 D. Y. Lyon, L. K. Adams, J. C. Falkner and P. J. J. Alvarez, *Environ. Sci. Technol.*, 2006, **40**, 4360-4366.

74 K. J. Moor, S. D. Snow and J.-H. Kim, *Environ. Sci. Technol.*, 2015, **49**, 5990-5998.

75 K. I. Priyadarsini, H. Mohan, A. K. Tyagi and J. P. Mittal, *J. Phys. Chem.*, 1994, **98**, 4756-4759.

76 Y. Yamakoshi, S. Sueyoshi, K. Fukuhara and N. Miyata, *J. Am. Chem. Soc.*, 1998, **120**, 12363–12364.

77 Y. Yoko, U. Naoki, R. Akemi, A. Kumi, M. Naoki, G. Yukihiro, M. Toshiki and T. Nagano, *J. Am. Chem. Soc.*, 2003, **125**, 12803-12809.

78 P. Mroz, G. P. Tegos, H. Gali, T. Wharton, T. Sarna and M. R. Hamblin, *Photochem. Photobiol. Sci.*, 2007, **6**, 1139-1149.

79 Z. Markovic and V. Trajkovic, *Biomaterials*, 2008, **29**, 3561-3573.

80 S. K. Sharma, L. Y. Chiang and M. R. Hamblin, *Nanomedicine*, 2011, **6**, 1813-1825.

81 Y. Yamazaki, A. A. Zinchenko and S. Murata, *Nanoscale*, 2011, **3**, 2909-2915.

82 Y.-Y Huang, S. K. Sharma, R. Yin, T. Agrawal, L. Y. Chiang and M. R. Hamblin, *J. Biomed. Nanotechnol.*, 2014, **10**, 1918-1936.

83 Y. Yamakoshi, S. Aroua, T.-M. D. Nguyen, Y. Iwamoto and T. Ohnishi, *Faraday Discuss.*, 2014, **173**, 287-296.

84 X. Liu, I. Que, X. Kong, Y. Zhang, L. Tu, Y. Chang, T. T. Wang, A. Chan, C. W. G. M. Löwikb and H. Zhang, *Nanoscale*, 2015, **7**, 14914-14923.

85 Y. Yang, M. Yu, H. Song, Y. Wang and C. Yu, *Nanoscale*, 2015, **7**, 11894-11898.

86 A. Soldà, A. Cantelli, M. Di Giosia, M. Montalti, F. Zerbetto, S. Rapino and M. Calvaresi, *J. Mater. Chem. B*, 2017, **5**, 6608-6615.

87 Y. Takano, R. Munechika, V. Biju, H. Harashima, H. Imahori and Y. Yamada, *Nanoscale*, 2017, **9**, 18690-18698.

88 R. Kumar, E. H. Gleißner, E. G. V. Tiu and Y. Yamakoshi, *Org. Lett.*, 2016, **18**, 184-187.

89 K. J. Moor and J.-H. Kim, *Environ. Sci. Technol.*, 2014, **48**, 2785-2791.

90 L. Ge, K. Moor, B. Zhang, Y. He and J.-H. Kim, *Nanoscale*, 2014, **6**, 13579-13585.

91 A. A. Ghogare and A. Greer, *Chem. Rev.*, 2016, **116**, 9994-10034.

92 S.-R. Chae, A. R. Badireddy, J. Farner Budarz, S. Lin, Y. Xiao, M. Therezien and M. R. Wiesner, *ACS Nano* 2010, **4**, 5011-5018.

93 E. M. Hotze, J. Labille, P. Alvarez and M. R. Wiesner, *Environ. Sci. Technol.*, 2008, **42**, 4175-4180.

94 M. Di Giosia, F. Valle, A. Cantelli, A. Bottoni, F. Zerbetto and M. Calvaresi, *Materials* 2018, **11**, 691